Journal of Structural Geology 32 (2010) 330–341

Contents lists available at ScienceDirect

Journal of Structural Geology

journal homepage: www.elsevier.com/locate/jsg

Numerical modeling of crenulation cleavage development: A polymineralic approach

Félice M.J. Naus-Thijssen*, Scott E. Johnson, Peter O. Koons

Department of Earth Sciences, University of Maine, 5790 Bryand Global Sciences Center, Orono, ME 04469, USA

ARTICLE INFO

Article history:
Received 9 July 2009
Received in revised form
10 December 2009
Accepted 4 January 2010
Available online 14 January 2010

Keywords:
Crenulation cleavage
Finite element analysis
Anisotropic elasticity
Pressure solution
OOF2

ABSTRACT

The finite element method was used to investigate how the elastic interactions of quartz and muscovite minerals affect grain-scale stress and strain distributions at different stages of crenulation cleavage development. The polymineralic structure comprises individual grains that were each assigned their own 3D stiffness tensor and orientation. Gradients in mean stress and volumetric strain within quartz grains develop between the limbs and hinges of microfolds at the earliest stages of crenulation development, with higher values in the microfold limbs. These gradients decrease with development of the crenulation cleavage, as the microfold limbs become phyllosilicate-rich (P) domains and the hinges become quartz- and feldspar-rich (QF) domains. Crystallographic orientations of the quartz grains have a relatively minor effect on the mean stress and volumetric strain distributions.

Our findings are broadly consistent with both pressure solution and strain-driven dissolution models for crenulation cleavage development. However, because crenulation cleavage development typically involves metamorphic reactions, we favor a model in which dissolution is driven by those reactions, and mass transfer leading to development of the mineralogically segregated fabric is driven by pore fluid pressure gradients that follow gradients in volumetric strain. Local concentrations of stress and strain across mineral interfaces may identify sites of enhanced reaction.

1. Introduction

Although crenulation cleavage is the most common type of cleavage in multiply-deformed, intermediate to high-grade metapelitic rocks (Williams et al., 2001), its formation and role in strain partitioning across a range of scales is incompletely understood. Crenulation cleavage is characterized by phyllosilicate-rich (P) domains, in which phyllosilicates define the overall cleavage, separated by quartz- and feldspar-rich (QF) domains (Fig. 1). Quartz grains in this fabric show little to no evidence for internal deformation or recrystallisation (Vernon and Clarke, 2008 and references therein). The characteristic mineralogical differentiation is therefore thought to result from dissolution of quartz and feldspar in the P-domains and precipitation of the dissolved material in the QF-domains (e.g. Gray and Durney, 1979; Schoneveld, 1979; Mancktelow, 1994). Alternatively, some percentage of the dissolved material may be removed from the local system (e.g. Bell et al., 1986; Wright and Henderson, 1992). There are two dominant hypotheses for crenulation cleavage formation. Pressure solution is most commonly invoked as the driving force for both dissolution and mass transfer from P-domains to QF-domains in both slaty cleavage (e.g. Sorby, 1863; Durney, 1972; Robin, 1979) and crenulation cleavage (e.g. Durney, 1972; Robin, 1979; Rutter, 1983). Pressure solution, sometimes referred to as dissolution or solution (-precipitation) creep or (stress-induced) dissolution and/or solution transfer, involves (1) the dissolution of material at grain boundaries that are subjected to a high normal stress, (2) diffusion of dissolved material down a chemical potential gradient induced by a gradient in normal stress, and (3) precipitation on open pore walls or within grain boundaries subjected to a lower normal stress. Strain-driven dissolution, where material moves from regions of high dislocation density to regions of low dislocation density, has been cited as an alternative to stress-induced dissolution (Bell et al., 1986; Vernon, 2004; Passchier and Trouw, 2005).

The influence of folding in a single or multilayered materials on stress and strain distributions, and how these distributions can be coupled to mass transfer, has been investigated numerically by a number of workers (e.g. Durney, 1978; Stephansson, 1974; Hobbs et al., 2000; Zhang et al., 2000). In these studies, folding of homogeneous layers is considered. However, rocks typically contain two or more minerals with variable geometrical and crystallographic arrangements relative to one another. The elastic interactions of

* Corresponding author. Fax: +1 207 581 2202.
E-mail address: felice.thijssen@umit.maine.edu (F.M.J. Naus-Thijssen).

0191-8141/$ – see front matter © 2010 Elsevier Ltd. All rights reserved.
doi:10.1016/j.jsg.2010.01.004

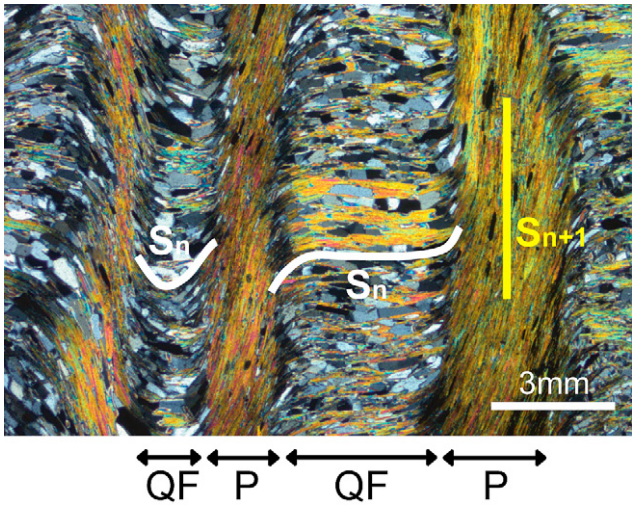

Fig. 1. Photomicrograph of crenulation cleavage. Indicated are the P- (crenulation limbs) and QF- (crenulation hinges) domains and two generations of foliation, S_n and S_{n+1}. Sample from the Main Central thrust zone, Nepal Himalaya.

these individual minerals lead to marked heterogeneity in the spatial distributions of stress and strain during deformation (e.g. Tullis et al., 1991; Johnson et al., 2004). Thus, the question arises as to how this grain-scale spatial heterogeneity will influence the larger scale (e.g. microfold half-wavelength) stress and strain gradients, and therefore the driving forces responsible for mass transfer during crenulation cleavage development. In order to examine grain-scale elastic interactions, we use the finite element method to evaluate instantaneous models containing hundreds of individual quartz and muscovite grains. Each grain is assigned its own crystallographic orientation and material-specific 3D stiffness tensor. The microstructure models are subjected to an elastic shortening strain of 1%. To evaluate how the spatial distributions and intensities of mechanical quantities change with fabric evolution, we consider three different stages of crenulation cleavage development (based on stages 2, 3 and 4 of Bell and Rubenach, 1983).

Below, we provide some background information on crenulation cleavage and its development. We then give background information and methodologies for our numerical experiments. Finally we discuss the results of our experiments and the implications for crenulation cleavage development. In summary, we find that mean stress and volumetric strain values in quartz grains vary systematically depending on domainal position within the crenulation cleavage microstructure. The resulting gradients between P- and QF-domains are consistent with a pressure solution mechanism of fabric formation, but they are also consistent with a formulation that emphasizes volumetric strains as opposed to stresses. The volumetric strain gradients are used as a proxy for how fluids will flow during fabric evolution, providing a quantitative basis for understanding mass transfer during crenulation cleavage development.

2. Background

2.1. General observations

Crenulation cleavage has been observed and described since the mid-19th century (e.g. Sharpe, 1849; Sorby, 1857, 1880), but it was not until the second half of the 20th century that workers began to systematically investigate the variables that determine its morphology and microstructure (e.g. Cosgrove, 1976; Gray, 1977a,b). The wide range of crenulation cleavage morphologies can be broadly subdivided into two classes: discrete and zonal crenulation cleavage. Both classes are gradational into one another and can occur together in one crenulated fabric (Gray, 1977a). Discrete crenulation cleavage refers to a crenulated fabric in which there are thin, sharply defined cleavage discontinuities (resembling microfaults or fractures) that truncate the pre-existing foliation. Zonal crenulation cleavage refers to a fabric in which the boundaries between the domains are gradational (e.g. Fig. 1). The general morphology of crenulation cleavage, regardless of whether it is discrete or zonal, is determined by the degree of mechanical anisotropy in the pre-existing fabric and the orientation of the fabric with respect to the maximum principal stress direction (e.g. Cosgrove, 1976; Gray, 1977b; Price and Cosgrove, 1990, p. 438). Crenulation cleavage folds may be symmetrical (e.g. Fig. 4, our model) or asymmetrical (e.g. Fig. 1), with the latter being the most common (Hobbs et al., 1976, p. 218) owing to the dominance of limbs over hinges in regionally folded rocks.

2.2. Previous modeling

The evolution of macro-, meso- and micro-scale folds, including the distributions of stress and strain within them, has been explored by theoretical (e.g. Biot, 1957, 1961; Ramberg, 1963; Johnson and Fletcher, 1994), analog (e.g. Ramberg, 1963; Means and Rogers, 1964; Means and Williams, 1972; Etheridge, 1973; Abbassi and Mancktelow, 1992) and numerical (e.g. Dieterich and Carter, 1969; Stephansson, 1974; Zhang et al., 2000; Hobbs et al., 2000) models.

In theoretical models, the formation of crenulation cleavage is divided into different stages. First, buckling instabilities are developed in an anisotropic medium, such as mineral fabrics or multilayered rocks. This is followed by the development of crenulation cleavage planes that are related to the microbuckles and are formed and further developed by a dissolution–precipitation process and mineral redistribution (e.g. Williams, 1972; Cosgrove, 1976; Gray and Durney, 1979). Bell and Rubenach (1983) proposed a six-stage model of crenulation cleavage development based on observations of both matrix and porphyroblast inclusion trails (Fig. 2). Stage 1 represents the initial homogeneous, planar foliation (S_n), which is gently crenulated in stage 2. At stage 3, solution- and precipitation-facilitated metamorphic differentiation occurs and a new foliation (S_{n+1}) begins to develop. At stage 4 new phyllosilicates grow parallel to S_{n+1}. At stage 5 a spaced cleavage develops in which the original fabric, S_n, is no longer visible. Eventually this spaced cleavage becomes homogenized at stage 6, resulting in a uniform, penetrative S_{n+1} schistosity.

In analog models with synthetic mica and artificial salt-mica schists conjugate shear zones with intervening microfolds that resemble crenulation cleavage structures were created (e.g. Means and Rogers, 1964; Means and Williams, 1972; Etheridge, 1973). In these experiments samples were compressed normal to the foliation to investigate the effects of strain rate, confining pressure and the role of water.

In numerical models single or multiple layers of elastic, viscous, elastic–viscous or elastic–plastic material containing small perturbations are embedded in a less competent matrix and subjected to shortening parallel to the layer(s) to investigate its/their behavior. These numerical models built upon theoretical models from Biot (e.g. Biot, 1957, 1959, 1961, 1964) and Ramberg (e.g. Ramberg, 1960, 1961, 1963) and analog models in which layers of materials like rubber sheets (e.g. Ramberg, 1961, 1963), plasticine (e.g. Cobbold et al., 1971) and wax (e.g. Abbassi and Mancktelow, 1992) were shortened. In multilayered systems asymmetric parasitic folds develop in the limbs, and symmetric folds develop in the hinge of

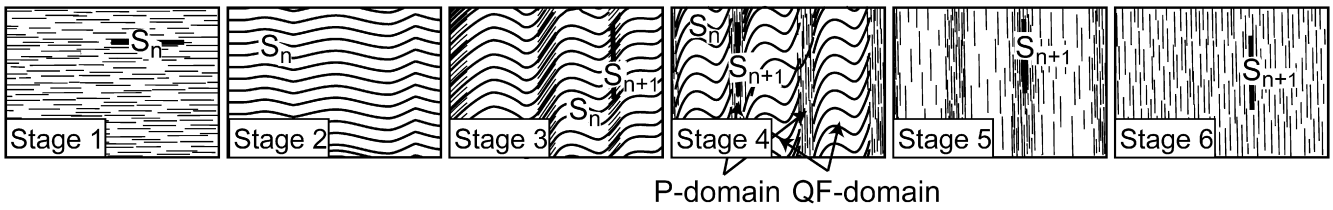

Fig. 2. Six stages of crenulation cleavage development. At stage 1 the original S_n foliation is present, which becomes crenulated at stage 2. At stage 3 the crenulation process is accompanied by solution/precipitation-facilitated metamorphic differentiation. At stage 4 new phyllosilicates begin to grow parallel to S_{n+1}. At stage 5 a spaced cleavage with no relic S_n in the QF-domains is formed that eventually becomes homogenized at stage 6. Modified from Bell and Rubenach (1983).

larger scale folds, similar to crenulation cleavage (Frehner and Schmalholz, 2006). The ratio of competency, or viscosity, between the different layers, and the strain rate at which the material is deformed, are important parameters determining the wavelength and periodicity of the folds (e.g. Biot, 1957; Hobbs et al., 2000; Zhang et al., 2000). Within the folded layers, mechanical disequilibria develop in the form of heterogeneous stress and strain distributions, causing free-energy gradients along which materials can diffuse (Stephansson, 1974). These gradients promote movement of material from the limb zones to the hinge zones of the folds and the variations of mean stress found in experimentally formed folds are consistent with variations in mineral composition, bulk chemical composition, and grain size of folds found in nature (e.g. Stephansson, 1974). More recent numerical models show a thermal–mechanical feedback, and explore the coupling of deformation to fluid flow and chemical reactions (Hobbs et al., 2008).

2.3. Mass transfer

Whether all of the material that is dissolved in the P-domains is precipitated in the QF-domains, or whether it is partly or entirely removed from the local system, is still a matter of debate. Most geochemical studies suggest that there is little to no volume loss in either low grade slaty cleavage or crenulation cleavage in higher grade rocks (e.g. Mancktelow, 1994; Erslev, 1998; Saha, 1998; McWilliams et al., 2007). Most microtextural and strain studies, on the other hand, suggest that dissolved material is removed from the system. Based on measurements of strain markers, volume losses of 50% or more are proposed in some slates (e.g. Wright and Henderson, 1992; Goldstein et al., 1995, 1998) and similar amounts have been postulated during the development of crenulation cleavage (Bell et al., 1986). The geochemical studies are based on the assumption that certain elements are immobile, serving as constants when comparing the compositions of different cleavage domains. Phyllosilicates that are not in equilibrium are also a base for assuming crenulation cleavage rocks are not part of a fluid-dominated system, and mass transfer is limited to a local scale (McWilliams et al., 2007). It also remains uncertain how much deformation has occurred in the "undeformed" reference domains used in these studies, adding to the issue of local compositional variations in sedimentary protoliths. The structural studies are based on the assumption that the original shapes and sizes of strain markers are well known. It is not yet clear which type of study – geochemical or structural – provides the more reliable results (e.g. Vernon, 1998; Williams et al., 2001).

3. Numerical modeling

3.1. Anisotropic elasticity

Although elastic anisotropy is considered as a material property in some of the models mentioned in the previous section, grain-to-grain interactions and the redistribution of grains are not; these factors may play an important role in driving mass transfer during crenulation cleavage formation. Gray and Durney (1979) discussed how different fabric-derived factors, namely grain shape, grain orientation, mineral solubility, grain boundary diffusion kinetics, grain contacts, and microfold wavelengths might affect crenulation cleavage differentiation. Below we investigate the influence of grain shape and orientation on microfolding and, in particular, crenulation cleavage development.

Because most minerals are elastically anisotropic, their shape and orientation influence the way in which they respond to an applied stress. This anisotropic behavior can be described (at low stress levels) with Hooke's law:

$$\sigma_{ij} = C_{ijkl}\varepsilon_{kl}, \quad (1)$$

where σ_{ij} is the stress, C_{ijkl} is the 4th rank elasticity tensor, and ε_{kl} is the strain (e.g. Nye, 1957). Assuming a 3D stress state, the elasticity tensor contains 81 elastic coefficients to link the stress tensor with the strain tensor. Each mineral has its own specific elasticity tensor. Due to the symmetry of the stress and strain tensors and the crystal symmetry of the minerals, the number of independent coefficients of the stiffness matrix (or elasticity tensor) can be simplified (Nye, 1957). Therefore, to describe the elasticity of muscovite, a monoclinic mineral, 13 independent elastic constants are needed, and quartz, a trigonal mineral, has 6 independent elastic constants (Fig. 3).

Experimental data on the compressibility of minerals show that muscovite is three to four times more compressible along the *c*-axis than along the *a*-axis or *b*-axis (Guidotti et al., 2005). For example, a Na-rich muscovite at room temperature and ~3.5 GPa will compress 3.59% along its *c*-axis and only 0.83% and 1.05% along its *a*-axis and *b*-axis, respectively (Comodi and Zanazzi, 1995). These numbers are sensitive to both temperature and composition. For quartz this difference is less pronounced: at the same conditions an α-quartz crystal will shorten 2.75% along its *a*-axes and 1.88% along its *c*-axis (Angel et al., 1997).

3.2. Method

In this study, the elastic interactions between individual muscovite and quartz grains and the influence of these interactions on stress and strain distributions within a rock are investigated by considering the crystallographic orientations and anisotropic elasticity of the individual grains. Simplified geometries, containing only quartz and muscovite grains, were created to represent three different stages of crenulation cleavage development (Fig. 4; based on stages 2–4 of Bell and Rubenach, 1983). The modal abundance of the two minerals is kept constant from stage to stage, implying that no material is lost during development. Although we have results for both symmetric and asymmetric crenulation cleavage, the results are similar so we only discuss the symmetric example.

Quartz

$$\begin{pmatrix} 86.6 & 6.7 & 12.6 & -17.8 & 0 & 0 \\ & (86.6) & (12.6) & (17.8) & 0 & 0 \\ & & 106.1 & 0 & 0 & 0 \\ & & & 57.8 & 0 & 0 \\ & & & & (57.8) & (-17.8) \\ & & & & & (39.95) \end{pmatrix}$$

Muscovite

$$\begin{pmatrix} 184.3 & 48.3 & 23.8 & 0 & -2 & 0 \\ & 178.4 & 21.7 & 0 & 3.9 & 0 \\ & & 59.1 & 0 & 1.2 & 0 \\ & & & 16.0 & 0 & 0.5 \\ & & & & 17.6 & 0 \\ & & & & & 72.4 \end{pmatrix}$$

Fig. 3. Stiffness matrix (Voigt notation) for Quartz and Muscovite in GPa at room temperature and atmospheric pressure. Data derived from Bass (1995).

OOF2 is a two-dimensional, object oriented finite element code developed by the National Institute of Standards and Technology (Langer et al., 2008; http://www.ctcms.nist.gov/oof/oof2/). The code uses image segmentation to divide an image into distinct sets of pixels that correspond to a homogeneous part of the image, i.e. the different grains (Reid et al., 2008). The different "pixel groups" are given their own material properties. In all models the muscovite grains are oriented with the *c*-axes parallel to the plane of the paper and perpendicular to the long dimension of the grain. Three variations of each of the three-modeled stages are evaluated in order to examine the role of quartz grain orientations on the solutions. In model I all quartz grains have the same orientation, with the *c*-axis (its least compliant axis) perpendicular to the plane of the paper. In model II all quartz grains have the same orientation, with the *c*-axis parallel to the shortening direction. In model III all the quartz grains have a random orientation. After defining the microstructure, a skeleton and mesh, composed of rectangular and triangular elements, are created (Fig. 5) using an auto-meshing option that automatically refines a skeleton until it fits the microstructure following a predefined set of operations that are described in Langer et al. (2008) and Reid et al. (2008). Models I and II consist of at least 10,000 elements and the models with the randomly oriented quartz consist of at least 16,000 elements. Once the mesh is defined, the models are subjected to 1% horizontal shortening. The upper and lower boundaries are defined as free surfaces (Fig. 5). Results are calculated in plane-strain, and values for mean stress and volumetric strain in response to the applied displacement at the boundaries are calculated and plotted.

For data analyses the model is divided into three different structural domains based on the orientations of the muscovite grains: P-, Q-, and X-domains (Fig. 4). In the P-domains, the long dimension of the muscovite grains are all oriented close to vertical and perpendicular to the shortening direction as is consistent with the P-domains in natural examples. In the Q-domains, all muscovite grains are oriented sub-horizontally, parallel to the shortening direction. In the X-domains, the long dimension of the muscovite grains are all oriented at an angle with respect to the shortening direction. The Q- and X-domains combined are equivalent to the QF-domains in natural examples.

3.3. Model results

3.3.1. Maps

Fig. 6 shows maps of the mean stress and the volumetric strain for the three stages of crenulation cleavage development, each subjected to a 1% horizontal shortening. This figure only shows the results for the model in which quartz grains are randomly oriented (model III); the effect of quartz orientation (the results of models I and II) will be discussed in Section 4.1. The muscovite grains in the Q- and P- domains show the most dramatic response to the deformation. In all stages, the muscovite grains in the Q-domain accommodate the highest compressive stresses and the lowest

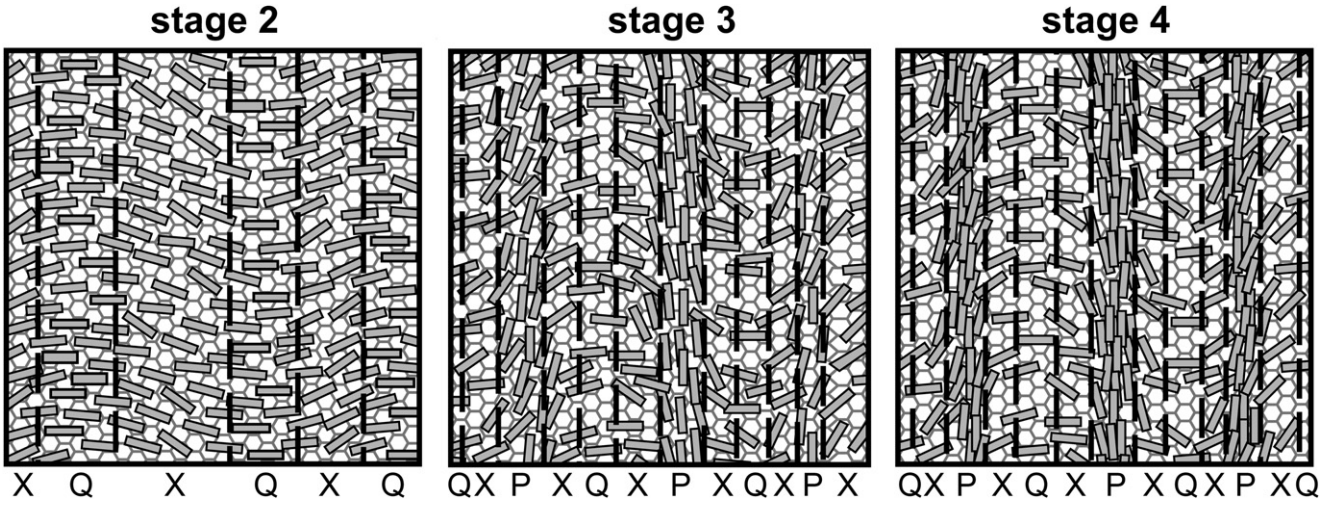

Fig. 4. Model setup. The grey rectangles represent muscovite grains and the grey lines outline the quartz grains. The *c*-axes of the muscovite grains are oriented perpendicular to the long axis of the grain and are parallel to the plane of the paper. The quartz grains are oriented differently in different models: they are oriented randomly (model III), with the *c*-axes perpendicular to the plane of the paper (model I), or with the *c*-axes parallel to the shortening direction (model II). The dashed lines outline the structural domains P, X and Q.

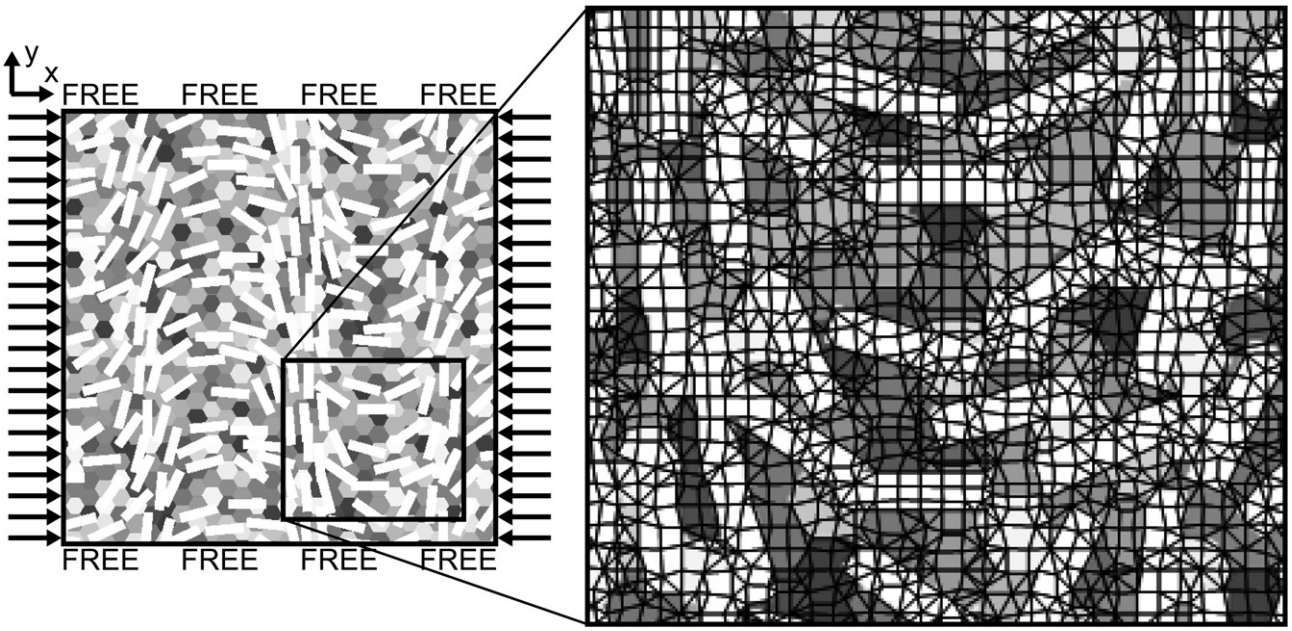

Fig. 5. Boundary conditions: each model is subjected to a horizontal shortening of 1%, the upper and lower boundaries are defined as free surfaces. The blowup image shows the mesh generated by OOF2.

negative volumetric strains. The muscovite grains in this domain are oriented with their least compliant axis (the *c*-axis) perpendicular to the shortening direction. In stages 3 and 4 the muscovite grains appear to act as stress beams, protecting the quartz grains from deformation in the Q-domains resulting in lower average mean stress and volumetric strain in quartz grains than in the P-domains. The highest negative volumetric strains are accommodated by the micas in the P-domains where the muscovite grains are oriented with their least compliant axis parallel to the shortening direction. The micas in the X-domains accommodate mean stresses intermediate between those in the P- and Q-domains and similar to the amounts accommodated by the quartz grains; these micas also accommodate low negative volumetric strains. Although the interaction among differently oriented quartz grains leads to local heterogeneity, domain-scale differences in mean stress and volumetric strain are established with higher values in the P-domains than in the X- and Q-domains. The magnitude of these gradients will be discussed in Section 3.3.2.

Mass transfer during crenulation cleavage development may be primarily driven by pore fluid pressure gradients, which we can approximate using gradients in the calculated volumetric strain field (e.g. Cox and Etheridge, 1989; Koons et al., 1998). To illustrate the general pattern of fluid flow, Fig. 7 shows a vector plot in which arrows are oriented down gradient, parallel to the local maximum gradient in volumetric strain. Although interaction among the different grains influences the direction of flow and complicates the local flow pattern, the domain-scale gradients in volumetric strain noted above lead to bulk flow from the P- and X- domains into the Q-domains. In natural examples, pathways for fluid flow would follow grain boundaries and possibly intragranular fractures. Thus, a more precise calculation of fluid flux would need to consider the geometry of these pathways (e.g. Carlson and Gordon, 2004; Joesten, 1991), but would not change our general result.

3.3.2. Statistical analysis of the data

In order to quantify the mean stresses and volumetric strains, average values and their standard deviations are calculated and plotted for quartz grains within the 3 structural domains (Fig. 8). The average values are calculated for only the quartz grains because quartz is the principle material that is dissolved, transferred, and precipitated. When comparing the models with the different orientations of quartz, model I accommodates the lowest mean stresses and highest negative volumetric strains, model II accommodates the highest mean stresses and lowest negative volumetric strains, and the model with the randomly oriented quartz grains (model III) shows intermediate values for mean stress and volumetric strain with respect to the other two models.

The skewness and kurtosis are calculated and plotted to give a measure of the variance of the datasets (Fig. 9). The datasets for the mean stress are slightly negatively skewed and have the highest kurtosis in the Q-domains. The skewness for the datasets of the volumetric strain differs from domain to domain: it is negative in the P-domains and positive or less negative in the other domains. The kurtosis for the data of the volumetric strain shows a slightly similar pattern as that of the kurtosis of the mean stress, with higher values of kurtosis in the Q-domains with respect to the other domains.

To give a better indication of the relative differences in mean stress and volumetric strain among the different domains the average values that are plotted in Fig. 8 are normalized against the average values in the Q-domains for each separate model. The greatest gradients (between the Q- and X-domains at stage 2, and between the Q- and X-domains at stages 3 and 4) are plotted in Fig. 10 and are largest at stage 2 for both the mean stress and the volumetric strain.

4. Discussion

4.1. Model results

A polymineralic approach has been used to model the incremental mean stress and volumetric strain distributions at three stages of crenulation cleavage development. We used finite element models composed of quartz and muscovite grains. The muscovite grains are all oriented with the *c*-axes parallel to the plane of the paper and perpendicular to the long dimension of

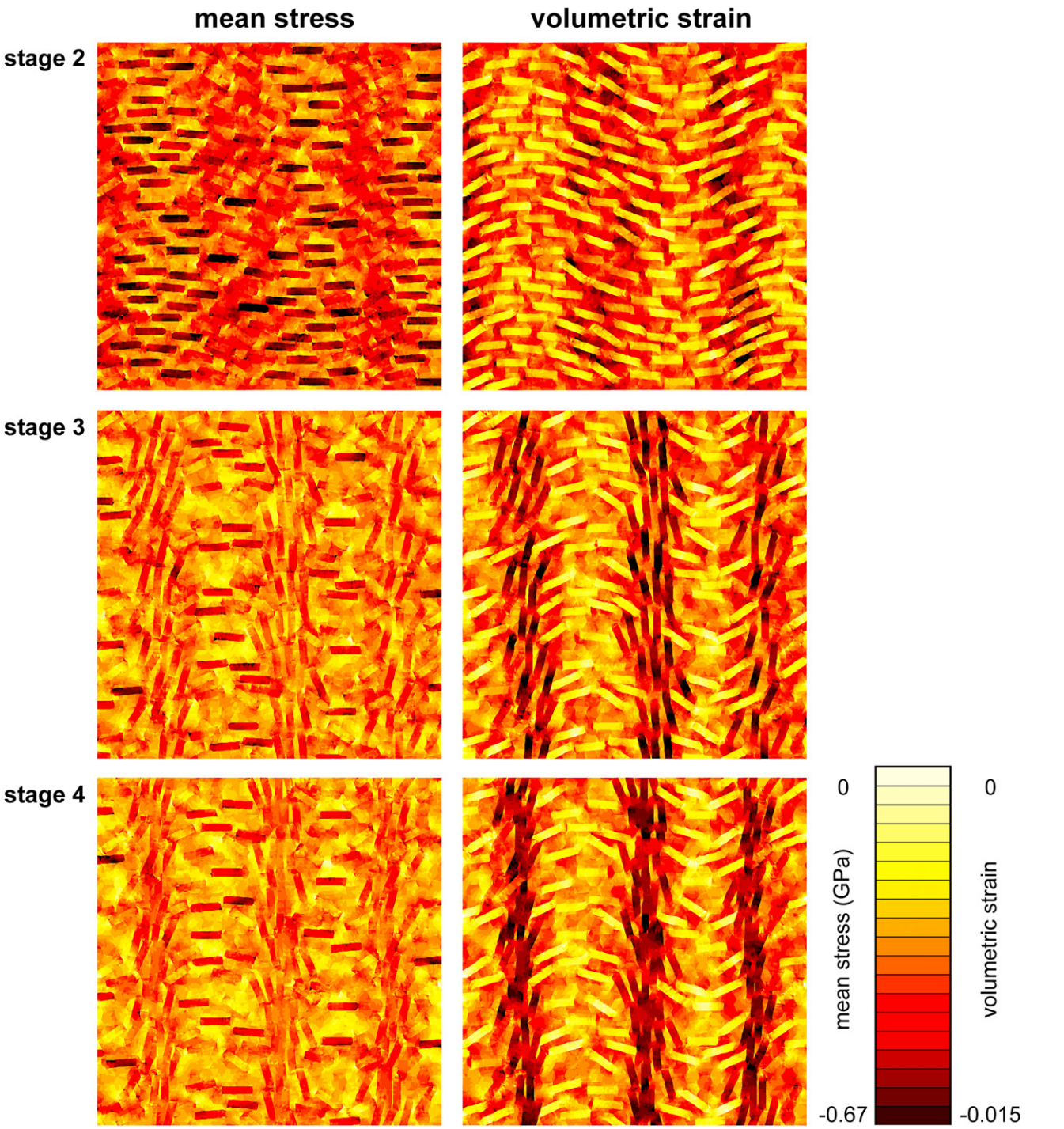

Fig. 6. Contour maps of the mean stress and volumetric strain for the three different stages of the model with the randomly oriented quartz grains (model III). Negative stress is compressional.

the grain. A distinction is made between three models based on the orientation of the quartz grains in the model: in models I and II the quartz grains all have the same orientation, with the *c*-axis perpendicular to the plane of the paper, or parallel to the shortening direction (model I and model II, respectively); in model III the quartz grains have a random orientation. Below we evaluate the influence of the orientation of the quartz grains, how the results differ from domain to domain and from stage to stage, and the distribution of the data.

4.1.1. Influence of the orientation of the quartz grains

The results show that there are no large differences between the three models (I, II and III) arising from the variation in quartz orientation (Fig. 8), confirming that the orientation and modal abundance of the muscovite grains plays the most important role in forming the overall stress and strain distributions in the developing crenulation cleavage fabric. The model containing randomly oriented quartz grains (model III) gives intermediate results for mean stress and volumetric strain. This is expected since the

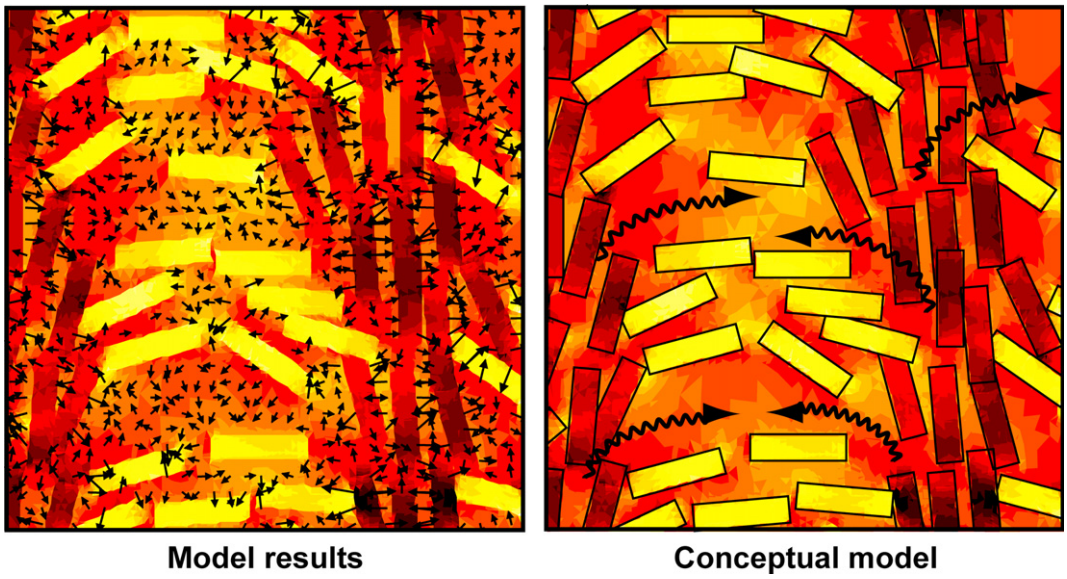

Fig. 7. Detail of the volumetric strain map from stage 3, model I. The arrows in the left image indicate mass transfer within the quartz (arrows originating in muscovite grains were removed from this flow chart). The origin of each arrow is the point of measurement. Arrows point toward the low negative volumetric strain regions. The length of the arrow indicates the magnitude of the gradient (short is a small gradient, long is a large gradient). The image on the right schematically shows the bulk flow from the P-domains to the QF-domains. Coloring is the same as in Fig. 6.

orientations of the quartz grains in the other two models represent the least compliant and one of the most compliant possible orientations for the quartz grains, relative to the applied shortening direction. In model III the quartz grains interact with one another creating a more heterogeneous pattern of stress and strain distribution, but the local high and low values appear to cancel each other out when calculating an average value per domain. Because the orientation of the quartz grains appears to play only a minor role in how mean stresses and volumetric strains are distributed, the results from model III will be used in the remainder of our discussion below.

4.1.2. Comparison of different domains and stages

Muscovite is elastically highly anisotropic, being more compressible along its c-axis and less compressible along its *a*-axis and *b*-axis than along any direction in quartz. In the P-domains, where the phyllosilicates are mainly oriented with their most compressible axis (sub-) parallel to the shortening direction, the quartz will always be the stiffest material. Thus, quartz in any orientation will carry higher mean stresses than the muscovite. In the Q-domains, where the phyllosilicates are oriented with their least compressible axes (sub-) parallel to the shortening direction, they are stiffer than quartz grains in any orientation, and will therefore carry higher mean stresses. In the X-domains an intermediate situation develops. The strong anisotropy of muscovite leads to less volumetric strain accumulation in quartz grains in the Q-domains compared to the quartz grains in the P-domains. Thus, we conclude that the systematic variation in muscovite orientation from P- to Q-domains causes the mean stress and volumetric strain gradients in quartz between these domains.

In all stages of crenulation cleavage development the mean stresses and volumetric strains are highest in the quartz grains in the P-domains (X-domains in stage 2) and lowest in the quartz grains in the Q-domains. The average values between those domains differ by up to 22% for both the mean stress and the volumetric strain and they decrease with fabric evolution (Fig. 10). At stage 2, P-domains have not yet developed, so more volumetric strain is accommodated in the quartz grains in the X-domains because there are no muscovite grains with their c-axes near-parallel to the shortening direction. As the fabric develops, muscovite grains rotate and recrystallize into more favorable orientations for strain in the P-domains, reducing the gradients at stage 3 relative to stage 2. At stage 4 there is modally less quartz in the P-domains and more quartz in the QX-domains than there is at stage 3, causing a slight increase in the gradients from stage 3 to stage 4.

4.1.3. Skewness and kurtosis of the data

The distributions (skewness and kurtosis) of the mean stress data show that most data points within the quartz in the different domains tend to have a low negative value (negative skewness) and less spread (peak of kurtosis) in the Q-domains than in the other domains. The latter pattern is due to the geometry of the Q-domains, which contain relatively more quartz than muscovite grains. Because there are fewer interactions between the two minerals this leads to a more homogeneous mean stress in the quartz. A similar pattern in kurtosis, although less pronounced, is found in the distributions of the volumetric strain data. The interactions between the individual quartz grains, causing heterogeneity in the stress and strain distributions, cause a shift from negative skewness in volumetric strain distribution in the P-domains to a positive or less negative skewness in the Q- and X-domains. The orientations of the muscovite grains have an important effect on the skewness: volumetric strains in the quartz grains tend to be on the higher (less negative) side if the phyllosilicates are oriented with their most compliant axis parallel to the shortening direction, and on the lower (more negative side) if the phyllosilicates are oriented with their most compliant axis perpendicular to the shortening direction.

4.2. Implications for crenulation cleavage development

The model results presented in this paper are based on instantaneous elastic interactions among quartz and muscovite grains at three different stages of crenulation cleavage development. No initial confining stresses are applied, and we do not consider time-

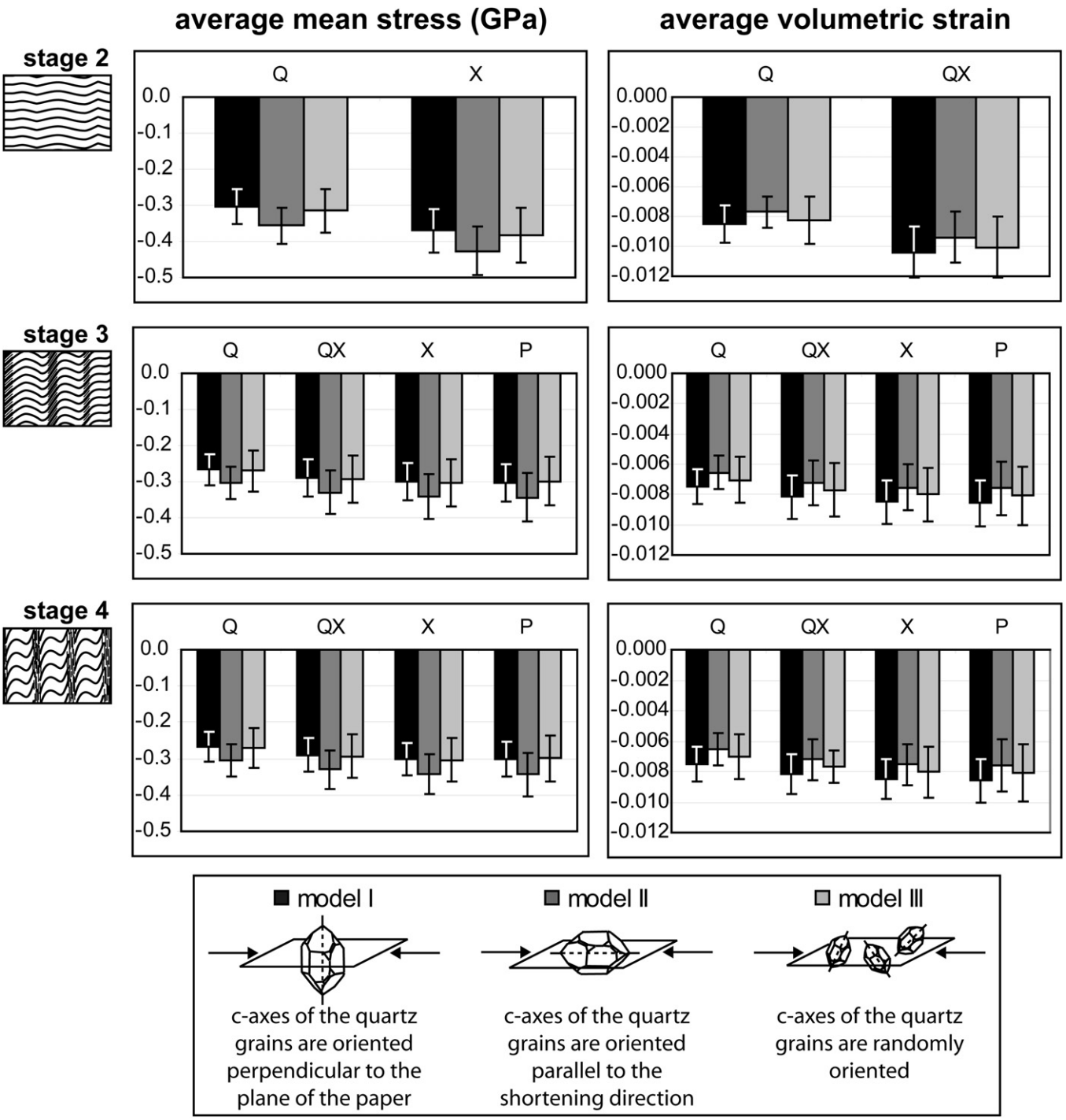

Fig. 8. Average mean stress and average volumetric strain in the quartz grains per structural domain. The bars represent plus and minus 1 standard deviation. For each domain the results for model III fall in between the results for models I and II. The values for the average mean stress and average volumetric strain are the lowest in the Q-domain at each stage.

and strain-dependent evolutionary processes such as grain boundary migration and dislocation creep, chemical reactions, and grain boundary diffusion and advection. Nevertheless, our results facilitate analysis of the stresses and strains that arise from elastic interactions of a polymineralic continuum, providing important constraints on the local and bulk stress and strain gradients that play a large role in establishing the characteristic mineralogical segregation associated with crenulation cleavage development.

The overall pattern of relatively high mean stresses in the quartz grains in the P-domains compared to those in the Q-domains is consistent with results derived from models in which homogeneous layers are folded (see Section 3.1). These folding models show the development of gradients in mean and normal stress between fold limbs and fold hinges, similar to those found in our results between P-domains and Q-domains in crenulation cleavage. Pressure solution has commonly been invoked in these folding models to relate the gradients in mean/normal stress to the transfer of quartz from the fold limbs to the fold hinges, not only in macroscale folds, but also in smaller scale crenulations. Similarly, Cosgrove (1976) suggested that the high stresses in the muscovite

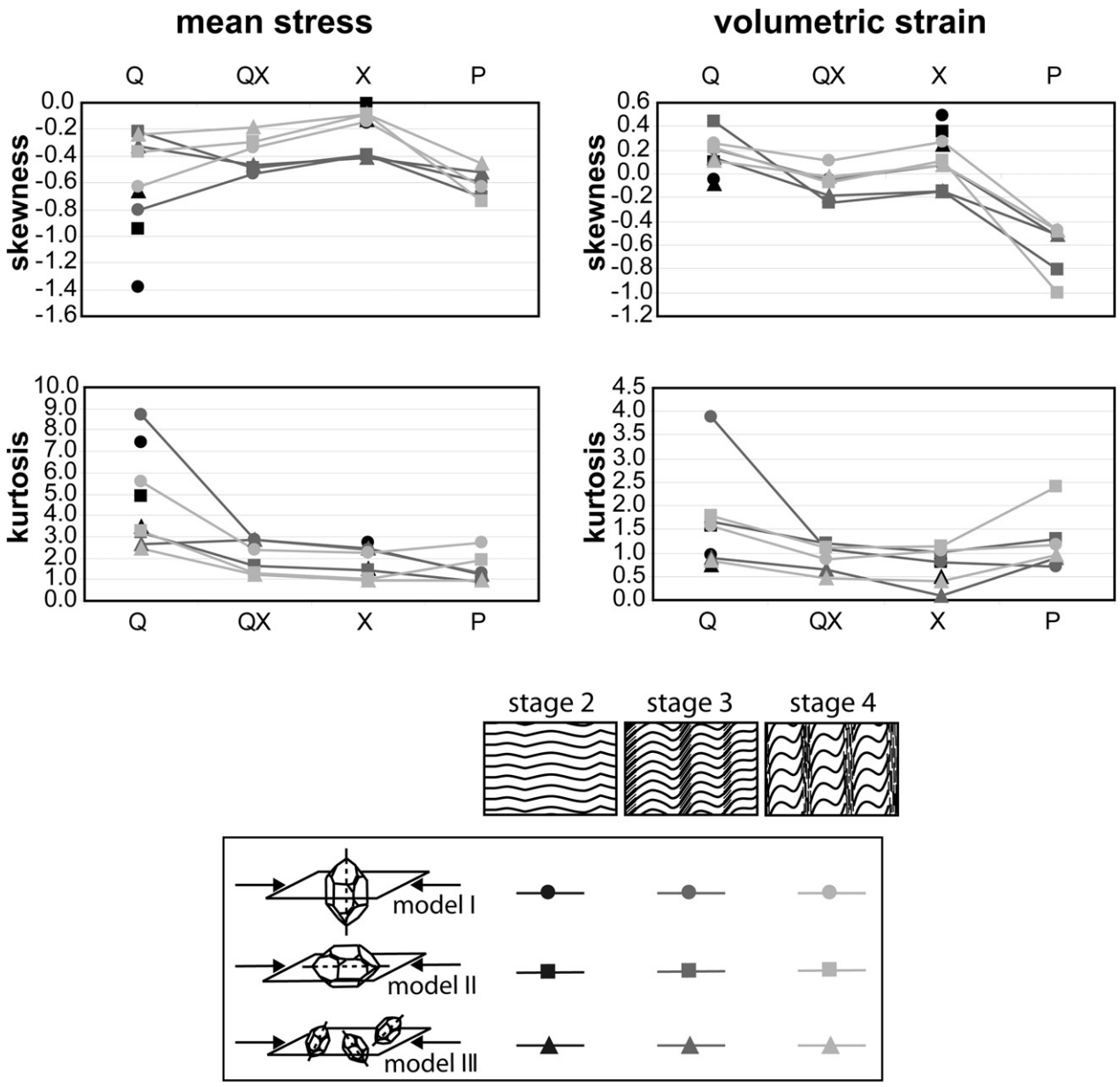

Fig. 9. Skewness and kurtosis of the mean stress and volumetric strain datasets. The mean stress data have negative skewness and a higher value of kurtosis in the Q-domains with respect to the kurtosis in the other domains. The volumetric strain data shift from a negative skewness in the P-domains to a less negative or positive skewness in the Q-domains. The volumetric strain data also show a peak of kurtosis in the Q-domains.

minerals in the QF-domains relative to the P-domains of crenulation cleavage should lead to the opposite, with dissolution of phyllosilicates in the QF-domains and their precipitation in the P-domains.

The role of pressure in the dissolution of quartz has been questioned (e.g. Bjørkum, 1996; Meyer et al., 2006). Field observations (e.g. Weyl, 1959; Houseknecht, 1988) and experimental work (e.g. Rutter and Wanten, 2000; Anzalone et al., 2006; Meyer et al., 2006) indicate that the presence of phyllosilicates enhance the dissolution of quartz. Bjørkum (1996) found very thin layers of mica or illite between two quartz grains and hypothesized that these thin layers could be missed, leading to a mistaken interpretation of pressure solution between two adjoining quartz grains (Bjørkum, 1996; Oelkers et al., 1996). Meyer et al. (2006) showed experimentally that dissolution of quartz is enhanced if in contact with muscovite in wet conditions (not under dry conditions) but slows down after time, possibly because of the reprecipitation of dissolved quartz outside the contact junction. Experimental data from Niemeijer and Spiers (2002) on the other hand showed no acceleration of compaction rates of quartz if muscovite was added. They postulated that dissolved Al^{3+} is responsible for decrease in solubility, dissolution rates, and precipitation rates of quartz. So, even though field data imply that the dissolution of quartz is enhanced by the presence of phyllosilicates, experimental data are still inconclusive and more investigations are required to evaluate the physics and chemistry of this process.

Experiments on quartz (Green, 1972; Hobbs, 1968), halite (Sprunt and Nur, 1977; Bosworth, 1981), and plagioclase (Kramer and Seifert, 1991) have shown that when these minerals are sufficiently strained, their solubility is enhanced due to an increase of dislocation density. Although Hirth and Tullis (1994) found similar results to Green (1972) for deformed quartz, they postulate that it is

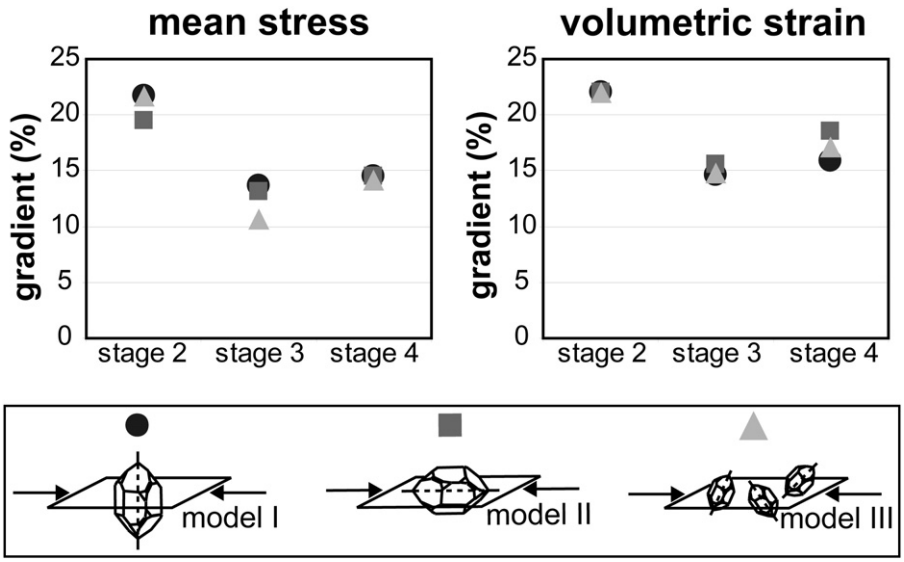

Fig. 10. Gradients between Q- and X- (stage 2) or P- (stage 3 and 4) domains in %. The gradient decreases from the early stage 2 to the intermediate stage 3 of crenulation cleavage development. At stage 4 the gradient increases slightly.

stress, and not the presence of a high dislocation density within the quartz, that causes the transition from α quartz to coesite. Bell et al. (1986) suggested that minerals like quartz and feldspars adjacent to phyllosilicates in rocks with crenulation cleavage, or metapelitic rocks in general, will be affected on their boundaries by shearing, increasing the dislocation energy, and enhancing the dissolution of those minerals. In this model, shear strain is accommodated by glide on the (001) planes in the phyllosilicates, whereas the quartz is plastically strained against the phyllosilicates on a variety of slip systems, generating a dislocation density gradient and eventually dissolves where the dislocation density is highest. However, the general lack of evidence for dislocation creep in quartz during crenulation cleavage development (Vernon and Clarke, 2008 and references therein) is difficult to reconcile with this model. Wintsch and Dunning (1985) calculated the energy stored in dislocations in quartz as a function of dislocation density and the effect of this increased energy on the activity of strained quartz and its solubility in pure H_2O. They found that the resulting increase in free energy is probably too small to play a significant geochemical role in rock deformation and hypothesized that where fluid/rock ratios are low, the aqueous activity of quartz might be significantly increased by the dissolution of quartz containing dislocation tangles, establishing a chemical potential gradient of SiO_2 and thus driving diffusive mass transfer, which is consistent with the results found in the experiments.

Fig. 11 shows a schematic diagram of fluid flow during crenulation cleavage formation, based on models from Bell and Hayward (1991) and Worley et al. (1997). Bell and Cuff (1989) argued that the anastomosing geometry of foliation generates areas of compression and tension, driving fluids towards localities of dilatation that are accommodated by microfracturing. These dilatational sites are formed preferentially in the extensional regions (QF-domains), and are proposed to be the nucleation sites for porphyroblasts. Worley et al. (1997) focused on the formation of discrete crenulation cleavage developed in chlorite- to garnet-zone schists. In order to explain the differences in mineralogy that they found in the different structural domains, they suggested that at early stages and chlorite zone conditions a zonal crenulation cleavage initially developed in response to microfolding and diffusive mass transfer at a local scale (less than half the wavelength of the crenulations). With progressive deformation a discrete crenulation cleavage evolved and these workers suggested that large-scale, buoyancy driven, advective flow occurred along the P-domains, in addition to grain boundary diffusion on a smaller scale.

A number of workers have investigated the role of metamorphic reactions during crenulation cleavage development (e.g. Marlow and Etheridge, 1977; Worley et al., 1997; Williams et al., 2001). They found that muscovite changes its composition in the P-domains and that plagioclase changes its composition in both the P- and QF-domains during foliation formation. This indicates that

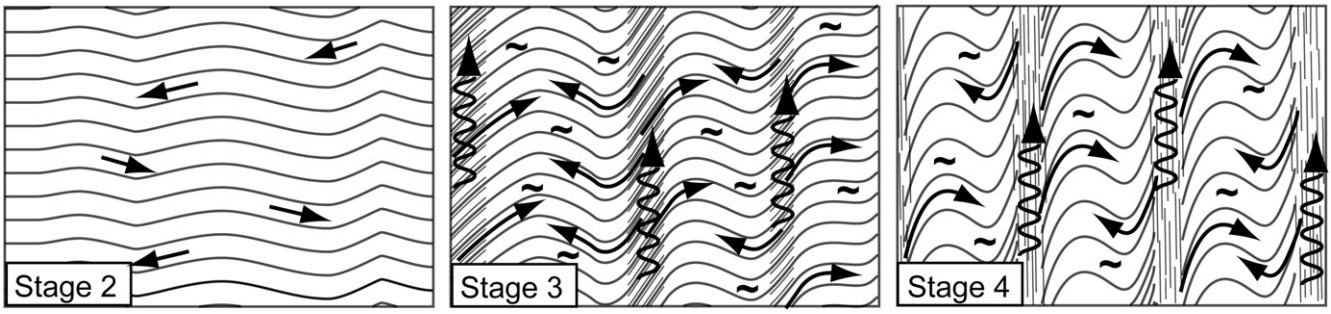

Fig. 11. Schematic diagram of fluid flow at stages 2, 3 and 4 of crenulation cleavage development based on models of Bell and Hayward (1991) and Worley et al. (1997). The arrows indicate fluid flow from P- to QF-domains, the wavy-arrows indicate fluid flow within the P-domains and the ~ indicate microfractures in the quartz.

metamorphic reactions play an important role during fabric development. It was implied that stress variations are not well assessed on the grain-size scale (Marlow and Etheridge, 1977) or are too small to drive dissolution and transportation of material, especially at elevated metamorphic grades (Williams et al., 2001). Both Marlow and Etheridge (1977) and Williams et al. (2001) suggested that metamorphic reactions are an important driving force for dissolution and that volumetric strain heterogeneities, determined by the microstructure of the fabric, might drive the mass transfer.

Our modeling results allow an evaluation of mineral-scale stress and strain heterogeneities and show that bulk flow driven by fluid pressure gradients will transfer soluble material from the P-domains into the QF-domains (Fig. 7). Because we do not consider mechanisms for viscous dissipation of elastic strain energy, the absolute values we obtained are not realistic for natural rocks. However, the relative values of stress and strain among the different domains are probably less susceptible to time-dependent decay and may be representative of natural conditions. Even though we do not find areas of dilatation in our models, the gradients in negative volumetric strain between the different structural domains (up to 22%) are probably sufficient to drive mass transfer, assuming that fluids are present and that pathways are available for fluid flow. Our results therefore support the suggestions of previous studies in which volumetric strain is considered to be important in mass transfer associated with crenulation cleavage. A model in which quartz is lost from the system (the modal abundance of quartz will decrease in the P-domains, but remain constant in the Q-domains) will generate different results from our isovolumetric model, but our general results pertaining to gradients in stresses and strains should still apply. Future work should examine time-dependent evolution of crenulation cleavage in which crystal plasticity (processes such as grain boundary migration and dislocation creep), chemical reactions, and diffusion and advection coupled to grain boundary structures are considered.

Given the observations made by us and others, and the model results presented here, we suggest that the most reasonable model for crenulation cleavage development is one in which metamorphic reactions drive the dissolution of material and variations in volumetric strain are largely responsible for transport of components from the P- to the QF-domains. This bulk transport is responsible for the characteristic mineralogical differentiation of crenulation cleavage. At the grain-scale, our model shows that there are large variations in mean stress and volumetric strain at grain interfaces, which are primarily controlled by the orientation of the phyllosilicate grains. These local variations may identify favorable sites for metamorphic reactions to initiate (de Ronde and Stünitz, 2007), but may also aid local diffusion and advection (Rutter, 1983; Etheridge and Hobbs, 1974).

5. Summary and conclusions

We used finite element techniques to evaluate the elastic stress and strain distributions at three instantaneous stages of crenulation cleavage development. Each model comprises hundreds of quartz and muscovite grains, and each grain was assigned its own 3D stiffness tensor and orientation. Each stage was subjected to a shortening of 1%. Our main findings are as follows.

(1) The orientation and distribution of muscovite grains are the primary factors determining how stress and strain are distributed within developing crenulation cleavage fabric. The orientations of the quartz grains are also important, but they play a subordinate role due to the extreme elastic anisotropy of the muscovite.

(2) Elastic mismatches between muscovite and quartz grains cause large variations in mean stress and volumetric strain intensity and distribution. Owing to the different orientations of muscovite grains in the different domains, crenulation-scale gradients are established with relatively high values of stress and volumetric strain on quartz grains in the P-domains and relatively low values on quartz grains in QF-domains. These gradients decrease as the fabric evolves into a fully developed crenulation cleavage.

(3) Although we cannot rule out either the pressure solution model or the strain-driven dissolution model, the evidence for metamorphic reactions in most crenulated rocks combined with our results support a model in which metamorphic reactions drive dissolution of material in the P-domains, and transportation to the QF-domains is driven by fluid pressure gradients that follow gradients in volumetric strain.

Acknowledgements

We gratefully acknowledge support for this work by the National Science Foundation, Grants EAR-0440063 and EAR-0236756, and a University of Maine Provost's Fellowship (to Naus-Thijssen). Stephen Langer and Andrew Reid of the National Institute of Standards and Technology are thanked for their help with OOF2 installation and troubleshooting. Discussions with Senthil Vel (UM Mechanical Engineering) were helpful in our analysis of the FEM results. Nancy Price is thanked for editing early versions of the manuscript. Special thanks to Mark Jessell and Albert Griera whose comments helped to improve the manuscript.

References

Abbassi, M.R., Mancktelow, N.S., 1992. Single layer buckle folding in non-linear materials – I. Experimental study of fold development from an isolated initial perturbation. Journal of Structural Geology 14, 85–104.
Angel, R.D., Allen, D.R., Miletich, R., Finger, L.W., 1997. The use of quartz as an internal pressure standard in high-pressure crystallography. Journal of Applied Crystallography 30, 461–466.
Anzalone, A., Boles, J., Greene, G., Young, K., Israelachvili, J., Alcantar, N., 2006. Confined fluids and their role in pressure solution. Chemical Geology 230, 220–231.
Bass, J.D., 1995. Elasticity of minerals, glasses, and melts. In: Ahrens, T.J. (Ed.), Mineral Physics and Crystallography. A Handbook of Physical Constants. AGU Reference Shelf 2. American Geophysical Union, Washington, D.C, pp. 45–63.
Bell, T.H., Rubenach, M.J., 1983. Sequential porphyroblast growth and crenulation cleavage development during progressive deformation. Tectonophysics 92, 171–194.
Bell, T.H., Cuff, C., 1989. Dissolution, solution transfer, diffusion versus fluid flow and volume loss during deformation or metamorphism. Journal of Metamorphic Geology 7, 425–447.
Bell, T.H., Hayward, N., 1991. Episodic metamorphic reactions during orogenesis: the control of deformation partitioning on reaction sites and reaction duration. Journal of Metamorphic Geology 9, 619–640.
Bell, T.H., Rubenach, M.J., Fleming, P.D., 1986. Porphyroblast nucleation, growth, and dissolution in regional metamorphic rocks as a function of deformation partitioning during foliation development. Journal of Metamorphic Geology 4, 37–67.
Biot, M.A., 1957. Folding instability of a layered viscoelastic medium under compression. Proceedings of the Royal Society of London A242, 444–454.
Biot, M.A., 1959. On the instability and folding deformation of a layered viscoelastic medium in compression. Journal of Applied Mechanics 26, 393–400.
Biot, M.A., 1961. Theory of folding of stratified viscoelastic media and its implications in tectonics and orogenesis. Geological Society of America Bulletin 72, 1595–1620.
Biot, M.A., 1964. Theory of internal buckling of a confined multilayered structure. Geological Society of America Bulletin 75, 563–564.
Bjørkum, P.A., 1996. How important is pressure in causing dissolution of quartz in sandstones. Journal of Sedimentary Research 66, 147–154.
Bosworth, W., 1981. Strain-induced preferential dissolution of halite. Tectonophysics 78, 509–525.
Carlson, W.D., Gordon, C.L., 2004. Effects of matrix grain size on the kinetics of intergranular diffusion. Journal of Metamorphic Geology 22, 733–742.
Cobbold, P.R., Cosgrove, J.W., Summers, J.M., 1971. Development of internal structures in deformed anisotropic rocks. Tectonophysics 12, 23–53.

Comodi, P., Zanazzi, P.F., 1995. High-pressure structural study of muscovite. Physics and Chemistry of Minerals 22, 170–177.
Cosgrove, J.W., 1976. The formation of crenulation cleavage. Journal of the Geological Society of London 132, 155–178.
Cox, S.F., Etheridge, M.A., 1989. Coupled grain-scale dilatancy and mass transfer during deformation at high fluid pressures: examples from Mount Lyell, Tasmania. Journal of Structural Geology 11, 147–162.
Dieterich, J.H., Carter, N.L., 1969. Stress-history of folding. American Journal of Science 267, 129–154.
Durney, D.W., 1972. Solution-transfer, an important geological deformation mechanism. Nature 235, 315–317.
Durney, D.W., 1978. A theory of mass-transfer-buckling deformation in finite amplitude sinusoidal multilayers. In: Easterling, K.E. (Ed.), Proceedings of the Interdisciplinary Conference held at the University of Lulea, Sweden, September 1978, pp. 393–405.
Erslev, E.A., 1998. Limited, localized nonvolatile element flux and volume change in Appalachian slates. Geological Society of America Bulletin 110, 900–915.
Etheridge, M.A., 1973. Experimentally produced slaty and crenulation cleavages during a single deformation. Journal of the Geological Society of Australia 20, 223–227.
Etheridge, M.A., Hobbs, B.E., 1974. Chemical and deformational controls on recrystallization of mica. Contributions to Mineralogy and Petrology 43, 111–124.
Frehner, M., Schmalholz, S.M., 2006. Numerical simulations of parasitic folding in multilayers. Journal of Structural Geology 28, 1647–1657.
Goldstein, A., Pickens, J., Klepeis, K., Linn, F., 1995. Finite strain heterogeneity and volume loss in slates of the Taconic Allochthon, Vermont, USA. Journal of Structural Geology 17, 1207–1216.
Goldstein, A., Knight, J., Kimball, K., 1998. Deformed graptolites, finite strain and volume loss during cleavage formation in rocks of the taconic slate belt, New York and Vermont, USA. Journal of Structural Geology 20, 1769–1782.
Gray, D.R., 1977a. Morphological classification of crenulation cleavage. Journal of Geology 85, 229–235.
Gray, D.R., 1977b. Some parameters which affect the morphology of crenulation cleavages. Journal of Geology 85, 763–780.
Gray, D.R., Durney, D.W., 1979. Crenulation cleavage differentiation: implications of solution-deposition processes. Journal of Structural Geology 1, 73–80.
Green II, H.W., 1972. Metastable growth of coesite in highly strained quartz. Journal of Geophysical Research 77, 2478–2482.
Guidotti, C.V., Sassi, F.P., Comodi, P., Zanazzi, P.F., Blencoe, J.G., 2005. Slaty cleavage: does the crystal chemistry of layer silicates play a role in its development? The Canadian Mineralogist 43, 311–325.
Hirth, G., Tullis, J., 1994. The brittle–plastic transition in experimentally deformed quartz aggregates. Journal of Geophysical Research 99, 11731–11747.
Hobbs, B.E., 1968. Recrystallization of single crystals of quartz. Tectonophysics 6, 353–401.
Hobbs, B.E., Means, W.D., Williams, P.F., 1976. An Outline of Structural Geology. John Wiley & Sons, Inc., New York.
Hobbs, B.E., Mühlhaus, H.B., Ord, A., Zhang, Y., Moresi, L., 2000. Fold geometry and constitutive behaviour. In: Jessell, M.W., Urai, J.L. (Eds.), Stress, Strain and Structure. A Volume in Honour of WD Means. Journal of the Virtual Explorer (online).
Hobbs, B., Regenauer-Lieb, K., Ord, A., 2008. Folding with thermal-mechanical feedback. Journal of Structural Geology 30, 1572–1592.
Houseknecht, D.W., 1988. Intergranular pressure solution in four quartzose sandstones. Journal of Sedimentary Petrology 58, 228–246.
Joesten, R., 1991. Grain-boundary diffusion kinetics in silicate and oxide minerals. In: Ganguly, J. (Ed.), Diffusion, Atomic ordering, and Mass transport, Selected Topics in Geochemistry. Spinger Verlag, pp. 345–395.
Johnson, A.M., Fletcher, R.C., 1994. Folding of Viscous Layers. Columbia University Press, New York.
Johnson, S.E., Vernon, R.H., Upton, P., 2004. Foliation development and progressive strain-rate partitioning in the crystallizing carapace of a tonalite pluton: microstructural evidence and numerical modeling. Journal of Structural Geology 26, 1845–1865.
Koons, P.O., Craw, D., Cox, S.C., Upton, P., Templeton, A.S., Chamberlain, C.P., 1998. Fluid flow during active oblique convergence: a Southern Alps model from mechanical and geochemical observations. Geology 26, 159–162.
Kramer, M.J., Seifert, K.E., 1991. Strain enhanced diffusion in feldspars. In: Ganguly, J. (Ed.), Diffusion, Atomic Ordering, and Mass Transport, Selected Topics in Geochemistry. Spinger Verlag, pp. 286–303.
Langer S.A., Reid A.C.E., Haan S.I., Garcia R.E., Lua R.C., Coffman V.R., 2008. The OOF2 Manual, Revision 3.7 for OOF2 Version 2.0.4.
Mancktelow, N.S., 1994. On volume change and mass transport during the development of crenulation cleavage. Journal of Structural Geology 16, 1217–1231.
Marlow, P.C., Etheridge, M.A., 1977. Development of a layered crenulation cleavage in mica schists of the Kanmantoo group near Macclesfield, South Australia. Geological Society of America Bulletin 97, 354–368.
McWilliams, C.K., Wintsch, R.P., Kunk, M.J., 2007. Scales of equilibrium and disequilibrium during cleavage formation in chlorite and biotite-grade phyllites, SE Vermont. Journal of Metamorphic Geology 25, 895–913.
Means, W.D., Rogers, J., 1964. Orientation of purophyllite synthesized in slowly strained materials. Nature 204, 244–246.
Means, W.D., Williams, P.F., 1972. Crenulation cleavage and faulting in an artificial salt-mica schist. Journal of Geology 80, 569–591.
Meyer, E.E., Greene, G.W., Alcantar, N.A., Israelachvili, J.N., Boles, J.R., 2006. Experimental investigation of the dissolution of quartz by a muscovite mica surface: implications for pressure solution. Journal of Geophysical Research 111, B08202.
Nye, J.F., 1957. Physical Properties of Crystals: Their Representation by Tensors and Matrices. Oxford University Press, London.
Niemeijer, A.R., Spiers, C.J., 2002. Compaction creep of quartz-muscovite mixtures at 500 °C: preliminary results on the influence of muscovite on pressure solution. In: de Meer, S., Drury, M.R., de Bresser, J.H.P., Pennock, G.M. (Eds.), Deformation Mechanisms, Rheology and Tectonics: Current Status and Future Perspectives. Geological Society of London, Special Publications, vol. 200, pp. 61–71.
Oelkers, E.H., Bjørkum, P.A., Murphy, W.M., 1996. A petrographic and computational investigation of quartz cementation and porosity reduction in North Sea sandstones. American Journal of Science 296, 420–452.
Passchier, C.W., Trouw, R.A.J., 2005. Microtectonics. Springer-Verlag.
Price, N.J., Cosgrove, J.W., 1990. Analysis of Geological Structures. Cambridge University Press.
Ramberg, H., 1960. Relationships between lengths of arc and thickness of ptygmatically folded veins. American Journal of Science 258, 36–46.
Ramberg, H., 1961. Contact strain and fold instability of a multilayered body under compression. Geologische Rundschau 51, 405–439.
Ramberg, H., 1963. Fluid dynamics of viscous buckling applicable to folding of layered rocks. Bulletin of the American Association of Petroleum Geologists 47, 484–505.
Reid, A.C.E., Langer, S.A., Lua, R.C., Coffman, V.R., Haan, S., Garcia, E.R., 2008. Image-based finite element mesh construction for material microstructures. Computational Materials Science 43, 989–999.
Robin, P.Y.F., 1979. Theory of metamorphic segregation and related processes. Geochimica et Cosmochimica Acta 43, 1587–1600.
de Ronde, A.A., Stünitz, H., 2007. Deformation-enhanced reaction in experimentally deformed plagioclase-olivine aggregates. Contributions to Mineralogy and Petrology 153, 699–717.
Rutter, E.H., 1983. Pressure solution in nature, theory and experiment. Journal of the Geological Society of London 140, 725–740.
Rutter, E.H., Wanten, P.H., 2000. Experimental study of the compaction of phyllosilicate-bearing sand at elevated temperature and with controlled pore water pressure. Journal of Sedimentary Research 70, 107–116.
Saha, D., 1998. Local volume change vs overall volume constancy during crenulation cleavage development in low grade rocks. Journal of Structural Geology 20, 587–599.
Schoneveld C., 1979. The geometry and the significance of inclusion patterns in syntectonic porphyroblasts. Ph.D. thesis, Universiteit Leiden, the Netherlands.
Sharpe, D., 1849. On slaty cleavage. Quarterly Journal of the Geological Society of London 5, 111–129.
Sorby, H.C., 1857. On some facts connected with slaty cleavage. British Association for the Advancement of Science Report 1857, 92–93.
Sorby, H.C., 1863. On the direct correlation of mechanical and chemical forces. Proceedings of the Royal Society of London 12, 538–550.
Sorby, H.C., 1880. On the structure and origin of non calcareous rocks. Proceedings of the Geological Society of London 36, 46–92.
Sprunt, E.S., Nur, A., 1977. Destruction of porosity through pressure solution. Geophysics 42, 726–741.
Stephansson, O., 1974. Stress-induced diffusion during folding. Tectonophysics 22, 233–251.
Tullis, T.E., Horowitz, F.G., Tullis, J., 1991. Flow laws of polyphase aggregates from end-member flow laws. Journal of Geophysical Research 96, 8081–8096.
Vernon, R.H., 1998. Chemical and volume changes during deformation and prograde metamorphism of sediments. In: Treloar, P.J., O'Brien, P.J. (Eds.), What drives Metamorphism and Metamorphic Reactions?. Geological Society of London, Special Publications, vol. 138, pp. 215–246.
Vernon, R.H., 2004. A Practical Guide to Rock Microstructure. Cambridge University Press, Cambridge, UK.
Vernon, R.H., Clarke, G.L., 2008. Principles of Metamorphic Petrology. Cambridge University Press.
Weyl, P.K., 1959. Pressure solution and the force of crystallization – a phenomenological theory. Journal of Geophysical Research 64, 2001–2025.
Williams, M.L., Scheltema, K.E., Jercinovic, M.J., 2001. High-resolution compositional mapping of matrix phases: implications for mass transfer during crenulation cleavage development in the Moretown Formation, western Massachusetts. Journal of Structural Geology 23, 923–939.
Williams, P.F., 1972. Development of metamorphic layering and cleavage in low grade metamorphic rocks at Bermagui, Australia. American Journal of Science 272, 1–47.
Wintsch, R.P., Dunning, J., 1985. The effect of dislocation density on the aqueous solubility of quartz and some geologic implications: a theoretical approach. Journal of Geophysical Research 90, 3649–3657.
Worley, B., Powell, R., Wilson, C.J.L., 1997. Crenulation cleavage formation: evolving diffusion, deformation and equilibration mechanisms with increasing metamorphic grade. Journal of Structural Geology 19, 1121–1135.
Wright, T.O., Henderson, J.R., 1992. Volume loss during crenulation cleavage formation in the Meguma Group, Nova Scotia, Canada. Journal of Structural Geology 14, 281–290.
Zhang, Y., Mancktelow, N.S., Hobbs, B.E., Ord, A., Mühlhaus, H.B., 2000. Numerical modelling of single-layer folding: clarification of an issue regarding the possible effect of computer codes and the influence of initial irregularities. Journal of Structural Geology 22, 1511–1522.